JOURNAL OF GUIDANCE, CONTROL, AND DYNAMICS
Vol. 15, No. 6, November-December 1992

Continuous Momentum Management of Earth-Oriented Spacecraft

John T. Harduvel*
McDonnell Douglas Space Systems Company, Huntington Beach, California 92647

A controller architecture is developed for momentum management of a control moment gyroscope controlled, Earth-oriented spacecraft that uses gravity gradient and aerodynamic torques generated by spacecraft maneuvering. Parameter selection within the architecture allows suppression of attitude or momentum variations due to constant and periodic disturbances as a function of frequency and axis. The capability provided to center the inertial components of the momentum vector reduces cyclic momentum use. An approximate closed-form solution for the "dynamic torque equilibrium attitude" (attitude motion requiring no control torque) and conditions for its existence are presented. The general three-axis coupled formulation of the governing equations includes aerodynamic torque derivative effects and permits momentum management of spacecraft with equal principal moments of inertia or orientations with significant pitch-to-roll/yaw coupling.

Nomenclature

C_j^k = direction cosine matrix transforming from frame j to frame k

Ω_{jk}^m = skew symmetric matrix form of ω_{jk}^m,

$$= \text{skew}[\omega_{jk}^m] = \begin{bmatrix} 0 & -\omega_{jk}^m(z) & \omega_{jk}^m(y) \\ \omega_{jk}^m(z) & 0 & -\omega_{jk}^m(x) \\ -\omega_{jk}^m(y) & \omega_{jk}^m(x) & 0 \end{bmatrix}$$

ω_{jk}^m = angular rate of frame k relative to frame j, components taken in frame m

$( )^m$ = vector or matrix coordinatized in the m frame

Subscripts and Superscripts

b = reference frame fixed relative to, but offset from, the body frame

body = body frame

i = inertial reference frame coincident with the n frame at time zero

n = local-vertical local-horizontal (LVLH) reference frame, x along the velocity vector, z down, and y forming an orthogonal right-handed set

p = principal axis reference frame

I. Introduction

SPACECRAFT that use control moment gyroscopes (CMGs) for attitude control must unload accumulated angular momentum to prevent saturation. Changing the momentum state of a spacecraft/CMG system requires applying an external torque. External torque can be produced by magnetic torquers, thrusters, gravity gradient torques, or aerodynamic torques. Methods that rely on only gravity gradient and/or aerodynamic torques generated by spacecraft maneuvers do not require consumables or additional hardware.

Shain and Spector[1] developed a continuous feedback controller architecture that integrates the functions of attitude control and momentum control using gravity gradient torques. They also provide compensation to decouple roll and yaw dynamics so that roll, pitch, and yaw controllers can be designed independently. This paper takes the opposite approach, designing a single controller that takes advantage of coupling between axes.

Wie et al.[2] incorporated "cyclic-disturbance rejection filters" in an integrated attitude/momentum controller. These filters are motivated by the fact that the natural environment in low Earth orbit for a spacecraft with articulated solar arrays is dominated by torque disturbances occurring at multiples of orbit frequency. In Ref. 2 it is seen that these filters suppress the effects of these disturbances on roll momentum, yaw attitude, and pitch attitude or momentum. They do not suppress roll attitude or yaw momentum at orbit frequency, nor do they suppress constant attitude offsets. The controller architecture presented here can suppress these states, with qualifications in some cases.

Warren et al.[3] present a method for "asymptotic momentum management" that lets the spacecraft assume a periodic attitude motion for which no control torque is required, i.e., a dynamic torque equilibrium attitude (TEA). The controller is configured to suppress CMG momentum in all axes at specific frequencies using disturbance rejection filters. For unchanging periodic disturbances, the result is a periodic spacecraft motion that (for a linear model) requires no CMG torque, even for unstable spacecraft dynamics. Conditions for the existence of the dynamic TEA are presented here.

Sunkel and Shieh[4,5] used the controller architecture in Ref. 2 and developed a method for placing the closed-loop poles of the controllers in a prescribed sector of the left-half plane.

All of the aforementioned references assume uncoupled roll/yaw and pitch dynamics to perform the controller designs, although Ref. 2 contains the coupled spacecraft dynamics equations. The uncoupled assumption is valid when the roll and yaw principal axes remain nearly parallel to the orbit plane and the aerodynamic torques are small. Some spacecraft may not satisfy this assumption, and in some cases it is advantageous to deliberately orient the spacecraft so that it violates this assumption.

In Refs. 1-5 aerodynamic torques are treated strictly as exogenous disturbances, invariant to spacecraft attitude changes. More accurate modeling of aerodynamic torques displays the dependence on attitude and therefore the ability of these torques to affect the stability of the system. Ignoring aerodynamic torque derivative effects in the controller analysis can result in poor performance or instability. The approach in Ref. 6 is limited to configuration control to achieve a stable aerodynamic equilibrium. However, when the aerodynamic torque derivatives are known, they can be manipulated just as gravity gradient torques and are not required to be stable.

Presented as Paper 90-3315 at the AIAA Guidance, Navigation, and Control Conference, Portland, OR, Aug. 20-22, 1990; received June 3, 1991; revision received March 10, 1992; accepted for publication March 27, 1992.

*Senior Specialist, Guidance, Navigation, and Control, Space Station Division, A95-J845-15/1, 5301 Bolsa Ave. Member AIAA.

The approaches taken in Refs. 1-5 mechanize either body or local-vertical local-horizontal (LVLH) integrals of in-the-orbit-plane momentum. The Ref. 2 approach, in addition, zeros the roll component of momentum. With the exception of Ref. 3, which implements the dynamic TEA, these do not zero the in-the-orbit-plane components of inertial momentum error. The controller architecture presented here does provide the option to zero the inertial zero-frequency components of steady-state momentum error.

This paper presents an approach to momentum management that accommodates three-axis coupled dynamics, includes aerodynamic torque derivative effects, and provides a general controller architecture allowing any possible blend of disturbance rejection filtering. Section II develops the equations of motion for an Earth-oriented, constant moment of inertia spacecraft coordinatized in the LVLH reference frame. Section III linearizes the equations. Section IV describes the controller architecture and discusses control options available to the designer, including the dynamic TEA. Section V presents several examples that demonstrate the important features of this controller architecture and the effects of aerodynamic torques.

II. Equations of Motion in the LVLH Frame

To design controllers for attitude control and momentum management, the spacecraft equations of motion are derived in the LVLH frame and linearized to obtain a dynamic model valid under the following assumptions:

1) The spacecraft is in a circular orbit:

$$\left(\omega^n_{\text{in}} = \begin{bmatrix} 0 \\ -\omega_o \\ 0 \end{bmatrix}, \qquad \omega_o = \text{constant orbital rate} \right)$$

2) The spacecraft moment of inertia tensor (J^b or J^{body}) is constant in a body-fixed frame.

3) The drag magnitude and the location of the aerodynamic center of pressure relative to the body frame are independent of spacecraft attitude.

4) Attitude motions relative to a reference orientation (operating point) are small.

5) Angular rates of the spacecraft relative to the LVLH frame are small compared to orbital rate: ($|\omega^n_{nb}(j)| \ll \omega_o$, $j = x,y,z$).

The angular momentum of the spacecraft in the inertial frame is

$$\boldsymbol{H}^i_{s/c} = C^i_n \boldsymbol{H}^n_{s/c} \tag{1}$$

Differentiating and equating to the total external torque gives

$$\boldsymbol{T}^i = \dot{\boldsymbol{H}}^i_{s/c} = \dot{C}^i_n \boldsymbol{H}^n_{s/c} + C^i_n \dot{\boldsymbol{H}}^n_{s/c} = C^i_n \Omega^n_{\text{in}} \boldsymbol{H}^n_{s/c} + C^i_n \dot{\boldsymbol{H}}^n_{s/c} \tag{2}$$

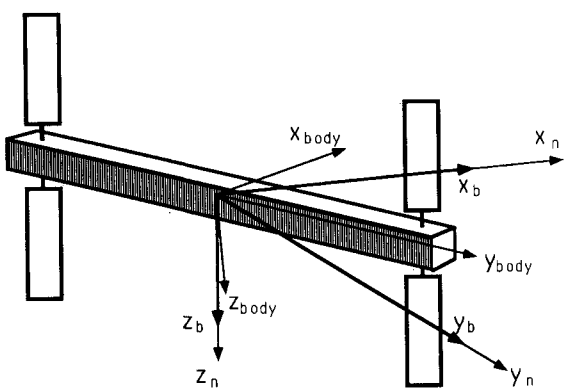

Fig. 1 Relationship between reference frames at the operating point.

Solving for $\dot{\boldsymbol{H}}^n_{s/c}$,

$$\dot{\boldsymbol{H}}^n_{s/c} = -\Omega^n_{\text{in}} \boldsymbol{H}^n_{s/c} + \boldsymbol{T}^n \tag{3}$$

The angular momentum of the spacecraft can be separated into a constant component (bias) plus a time-varying component:

$$\boldsymbol{H}^n_{s/c}(t) = \bar{\boldsymbol{H}}^n_{s/c} + \Delta \boldsymbol{H}^n_{s/c}(t) \tag{4}$$

so that

$$\Delta \dot{\boldsymbol{H}}^n_{s/c} = -\Omega^n_{\text{in}} \Delta \boldsymbol{H}^n_{s/c} - \Omega^n_{\text{in}} \bar{\boldsymbol{H}}^n_{s/c} + \boldsymbol{T}^n \tag{5}$$

The total torque on the spacecraft includes contributions due to gravity gradient $\boldsymbol{T}_{gg}$, other external disturbances $\boldsymbol{T}_d$, and the control $\boldsymbol{T}_c$:

$$\boldsymbol{T}^n = \boldsymbol{T}^n_{gg} + \boldsymbol{T}^n_d + \boldsymbol{T}^n_c \tag{6}$$

The gravity gradient torque in the LVLH frame is given by

$$\boldsymbol{T}^n_{gg} = 3\omega_o^2 \begin{bmatrix} 0 & 1 & 0 \\ -1 & 0 & 0 \\ 0 & 0 & 0 \end{bmatrix} J^n \begin{bmatrix} 0 \\ 0 \\ -1 \end{bmatrix} \tag{7}$$

where ω_o is the spacecraft orbital rate and J^n the spacecraft moment of inertia (MOI) tensor expressed in the LVLH frame.

The external disturbance torque consists of a component along the velocity vector, $T^n_{dx}(t)$, which is assumed invariant with spacecraft attitude θ, and components orthogonal to it, $T^n_{dy}(t,\theta)$ and $T^n_{dz}(t,\theta)$, representing aerodynamic torques due primarily to drag. Let $\boldsymbol{r}_{cp}(t)$ be the vector distance from the center of mass to the center of pressure, and $\boldsymbol{D}(t)$ be the aerodynamic drag force on the spacecraft. The disturbance torque due to aerodynamic drag is

$$\begin{bmatrix} 0 \\ T^n_{dy}(t,\theta) \\ T^n_{dz}(t,\theta) \end{bmatrix} = \boldsymbol{r}^n_{cp}(t) \times \boldsymbol{D}^n(t) = \left[C^n_b(\theta) \;\; \boldsymbol{r}^b_{cp}(t) \right] \times \boldsymbol{D}^n(t) \tag{8}$$

where the selection of reference frame b and its relationship to θ are discussed in Sec. III.

The attitude of the spacecraft relative to the LVLH frame is computed by integrating

$$\dot{C}^n_b = \Omega^n_{nb} C^n_b \tag{9}$$

where $\Omega^n_{nb} = \text{skew}[\omega^n_{nb}]$, and

$$\omega^n_{nb} = [J^n]^{-1}(\bar{\boldsymbol{H}}^n_{s/c} + \Delta \boldsymbol{H}^n_{s/c}) - \omega^n_{\text{in}} \tag{10}$$

The CMG momentum dynamics are defined by

$$\dot{\boldsymbol{h}}^n_c = -\Omega^n_{\text{in}} \boldsymbol{h}^n_c - \boldsymbol{T}^n_c \tag{11}$$

where $\boldsymbol{h}^n_c$ is the angular momentum vector of the CMGs, components in the LVLH frame.

III. Linearization of the Equations of Motion

The equations are to be linearized about the operating point $\Delta \boldsymbol{H}^n_{s/c} = 0$ and $C^n_b = I$, where I is the 3×3 identity matrix. The b frame is defined as fixed in the spacecraft and coincident with the n frame at the operating point, as illustrated in Fig. 1. The b frame is related to the body frame by the constant transformation C^b_{body} so that $J^b = C^b_{\text{body}} J^{\text{body}} C^{\text{body}}_b = \text{const}$. There are no small angle restrictions on C^b_{body}.

In order to have $\Delta \boldsymbol{H}^n_{s/c} = 0$ at the operating point, the constant $\bar{\boldsymbol{H}}^n_{s/c}$ is defined as $\bar{\boldsymbol{H}}^n_{s/c} \triangleq J^b \omega^n_{\text{in}}$.

The attitude of the spacecraft is assumed to deviate from the operating point by small angles $\theta^n_{nb} = [\theta_x, \theta_y, \theta_z]^T$; thus, the following approximations are valid. (Recall that arbitrarily large angles are permitted between the body or principal axes and LVLH.) Let $\Theta = \text{skew}[\theta^n_{nb}]$ so that

$$C^n_b \cong I + \Theta \tag{12}$$

Then

$$J^n \cong (I+\Theta)J^b(I-\Theta) \cong J^b + \Theta J^b - J^b\Theta \tag{13}$$

and

$$[J^n]^{-1} \cong [J^b]^{-1} + \Theta[J^b]^{-1} - [J^b]^{-1}\Theta \tag{14}$$

The approximation for the gravity gradient torque as a linear function of attitude is obtained by substituting Eq. (13) into Eq. (7):

$$T^n_{gg} \cong 3\omega_o^2 \begin{bmatrix} -J_{23} \\ J_{13} \\ 0 \end{bmatrix} + 3\omega_o^2 \begin{bmatrix} (J_{33}-J_{22}) & J_{12} & -J_{13} \\ J_{12} & (J_{33}-J_{11}) & -J_{23} \\ 0 & 0 & 0 \end{bmatrix} \begin{bmatrix} \theta_x \\ \theta_y \\ \theta_z \end{bmatrix} \tag{15}$$

where the J are the elements of the symmetric matrix J^b.

To obtain the linearized equation for the aerodynamic torque, let $r^b_{cp}(t) = [r_x(t), r_y(t), r_z(t)]^T$ and $D^n = [D(t), 0, 0]^T$. Since we desire a linear time-invariant system of equations, we will use the average value of the aerodynamic torque over one orbit for the system matrix portion of the result. Substituting Eq. (12) into Eq. (8) and rearranging gives

$$\begin{bmatrix} 0 \\ T^n_{dy}(t,\theta) \\ T^n_{dz}(t,\theta) \end{bmatrix} \cong \begin{bmatrix} 0 \\ r_z(t)D(t) \\ -r_y(t)D(t) \end{bmatrix} + \begin{bmatrix} 0 & 0 & 0 \\ -\bar{t}_{dz} & -\overline{r_xD} & 0 \\ \bar{t}_{dy} & 0 & -\overline{r_xD} \end{bmatrix} \begin{bmatrix} \theta_x \\ \theta_y \\ \theta_z \end{bmatrix} \tag{16}$$

where

$$\bar{t}_{dy} = \omega_o/2\pi \int_0^{2\pi/\omega_o} r_z(t)D(t)\,dt$$

$$\bar{t}_{dz} = \omega_o/2\pi \int_0^{2\pi/\omega_o} -r_y(t)D(t)\,dt$$

$$\overline{r_xD} = \omega_o/2\pi \int_0^{2\pi/\omega_o} r_x(t)D(t)\,dt$$

The total disturbance as a linear function of attitude is then

$$T^n_d(t,\theta) = \begin{bmatrix} T^n_{dx}(t) \\ T^n_{dy}(t) \\ T^n_{dz}(t) \end{bmatrix} + \begin{bmatrix} 0 & 0 & 0 \\ -\bar{t}_{dz} & -\overline{r_xD} & 0 \\ \bar{t}_{dy} & 0 & -\overline{r_xD} \end{bmatrix} \begin{bmatrix} \theta_x \\ \theta_y \\ \theta_z \end{bmatrix} \tag{17}$$

The final expression for $\Delta\dot{H}^n_{s/c}$ is obtained by substituting Eqs. (6), (15), and (17) into Eq. (5):

$$\Delta\dot{H}^n_{s/c} = A_{H\theta}\theta^n_{nb} - \Omega^n_{\text{in}}\Delta H^n_{s/c} + T^n_c + T^n_d(t) + \omega_o^2 \begin{bmatrix} -4J_{23} \\ 3J_{13} \\ J_{12} \end{bmatrix} \tag{18}$$

Table 1 Phase I space station MOI and disturbance environment data

$$J^{\text{body}} = \begin{bmatrix} 50.28 & -0.39 & 0.16 \\ -0.39 & 10.80 & 0.16 \\ 0.16 & 0.16 & 58.57 \end{bmatrix} \times 10^6 \quad \text{slug-ft}^2$$

$$T^{\text{body}}_d(t) = \begin{bmatrix} 1 \\ 4 \\ 1 \end{bmatrix} + \begin{bmatrix} 1 \\ 2 \\ 1 \end{bmatrix} \sin(\omega_o t) + \begin{bmatrix} 0.5 \\ 0.5 \\ 0.5 \end{bmatrix} \sin(2\omega_o t) \quad \text{ft-lb}^a$$

$\omega_o = 0.0011$ rad/s

[a]Disturbance environment applies when body axes are coincident with LVLH axes.

where

$$A_{H\theta} = \begin{bmatrix} 3(J_{33}-J_{22})\omega_o^2 & 3J_{12}\omega_o^2 & -3J_{13}\omega_o^2 \\ 3J_{12}\omega_o^2 - \bar{t}_{dz} & 3(J_{33}-J_{11})\omega_o^2 - \overline{r_xD} & -3J_{23}\omega_o^2 \\ \bar{t}_{dy} & 0 & -\overline{r_xD} \end{bmatrix}$$

The matrix $A_{H\theta}$ is extremely important because it determines what motions can be used for momentum control. The selected motions must be capable of producing a sufficient torque both in the orbit plane (LVLH x or z axis) and normal to the orbit plane (LVLH y axis). The presence of the $\bar{t}_{dy}$, $\bar{t}_{dz}$, and $\overline{r_xD}$ terms in $A_{H\theta}$ means that the aerodynamic disturbances affect the system eigenvalues, and whenever they are significant they must be included in the linearized model used for control system analysis. Furthermore, as Sec. V demonstrates, when these terms are known to sufficient accuracy, the controller can take advantage of these terms to aid in, or be the primary source of, momentum control.

The rate of change of attitude error is obtained as a linear function of θ^n_{nb} and $\Delta H^n_{s/c}$ by substituting Eqs. (10), (12), and (14) into Eq. (9) and retaining first-order terms:

$$\dot{\theta}^n_{nb} = A_{\theta\theta}\theta^n_{nb} + [J^b]^{-1}\Delta H^n_{s/c} \tag{19}$$

where

$$A_{\theta\theta} = [J^b]^{-1}\,\text{skew}[\bar{H}^n_{s/c}] - \Omega^n_{\text{in}} \tag{20}$$

The plant linearized equations of motion are now complete and defined by Eqs. (11), (18), and (19).

IV. Controller Architecture

Given the plant linearized equations of motion developed in Sec. III, a controller architecture for simultaneous attitude and momentum control follows. The plant state equations are augmented with integrators and a general formulation of disturbance rejection filters that enable a feedback controller to drive specific frequency components of linear combinations of plant states to zero. These integrators and filters can be used to impose constraints on the spacecraft motion, minimize attitude errors, minimize CMG momentum, or achieve a desired ratio between attitude error and momentum. The filters are set to multiples of orbit frequency to suppress disturbances arising from the natural environment.

The external torques generated to control momentum must include inertial zero-frequency components both in, and normal to, the orbit plane that cancel the secular components of disturbances. When viewed in the LVLH frame, the inertial in-plane component appears sinusoidal at orbit frequency. Any spacecraft motions that can produce sufficient torques of this kind can be used to control momentum. When either aerodynamic torques or the spacecraft products of inertia in the LVLH frame are significant, an infinite set of motions exist

that produce the required external torque. This is because three degrees of freedom are available at zero frequency to satisfy one torque equilibrium equation normal to the orbit plane and six degrees of freedom are available at orbit frequency to satisfy two torque equilibrium equations in the orbit plane.

The following controller architecture accommodates any of these motions for momentum management and allows the designer to selectively suppress the effects of disturbances in either attitude or momentum at each frequency (0, ω_o, and $2\omega_o$) and in each axis.

The augmented system state equation and controller are defined by

$$\frac{\mathrm{d}}{\mathrm{d}t}\begin{bmatrix} \boldsymbol{h}_c^n \\ \theta_{nb}^n \\ \Delta \boldsymbol{H}_{s/c}^n \\ \boldsymbol{f0} \\ \boldsymbol{f1}_1 \\ \boldsymbol{f1}_2 \\ \boldsymbol{f2}_1 \\ \boldsymbol{f2}_2 \end{bmatrix} = \begin{bmatrix} -\Omega_{\text{in}}^n & 0 & 0 & 0 & 0 & 0 & 0 & 0 \\ 0 & A_{\theta\theta} & [J^b]^{-1} & 0 & 0 & 0 & 0 & 0 \\ 0 & A_{H\theta} & -\Omega_{\text{in}}^n & 0 & 0 & 0 & 0 & 0 \\ A_{0h} & A_{0\theta} & 0 & 0 & 0 & 0 & 0 & 0 \\ A_{11h} & A_{11\theta} & 0 & 0 & 0 & \omega_o I & 0 & 0 \\ A_{12h} & A_{12\theta} & 0 & 0 & -\omega_o I & 0 & 0 & 0 \\ A_{21h} & A_{21\theta} & 0 & 0 & 0 & 0 & 0 & 2\omega_o I \\ A_{22h} & A_{22\theta} & 0 & 0 & 0 & 0 & -2\omega_o I & 0 \end{bmatrix} \begin{bmatrix} \boldsymbol{h}_c^n \\ \theta_{nb}^n \\ \Delta \boldsymbol{H}_{s/c}^n \\ \boldsymbol{f0} \\ \boldsymbol{f1}_1 \\ \boldsymbol{f1}_2 \\ \boldsymbol{f2}_1 \\ \boldsymbol{f2}_2 \end{bmatrix} + \begin{bmatrix} -I \\ 0 \\ I \\ 0 \\ 0 \\ 0 \\ 0 \\ 0 \end{bmatrix} T_c^n + \begin{bmatrix} 0 \\ 0 \\ I \\ 0 \\ 0 \\ 0 \\ 0 \\ 0 \end{bmatrix} \left\{ T_d^n(t) + \omega_o^2 \begin{bmatrix} -4J_{23} \\ 3J_{13} \\ J_{12} \end{bmatrix} \right\} \tag{21}$$

and

$$T_c^n = -Kx \tag{22}$$

where $I = 3 \times 3$ identity matrix, K is a 3×24 gain matrix, and x is the state vector of Eq. (21).

The f in Eq. (21) are filter states whose derivatives are definable using the rows of the 3×3 submatrices A_{ih} and $A_{i\theta}$, $i = 0, 11, 12, 21, 22$. The designer defines the rows of A_{ih} and $A_{i\theta}$ as vectors in the direction of momentum error vectors or attitude error vectors, respectively, that are to be nulled in steady state. The $f0$ allows three vectors to be nulled at zero frequency (DC), the $f1$ allow three vectors to be nulled at ω_o, and the $f2$ allow three vectors to be nulled at $2\omega_o$. Additional filters could be added at other frequencies if required. The designer may also null weighted combinations of attitude and momentum vectors to achieve a desired tradeoff by including entries in the same row of A_{ih} and $A_{i\theta}$.

The $f0$ filters can be used to maintain zero attitude error or zero momentum error (which defines the zero-frequency TEA) at zero frequency in any axis. In normal situations, requiring all attitude errors to be zero at zero frequency will prohibit CMG momentum control normal to the orbit plane. Nevertheless, this can be accomplished if unbounded CMG momentum growth is temporarily allowed and requires all gains multiplying LVLH y axis CMG momentum to be zero. Likewise, requiring all attitude errors to be zero at orbit frequency will also result in unbounded momentum growth, and requires all gains multiplying LVLH x and z axis CMG momentum to be zero. All attitude errors may be made zero at any other frequency resulting in only cyclic momentum use.

Although the $f1$ are second-order filters in the LVLH frame, they can also be used to perform inertial integration of LVLH frame in-plane states. To see this, consider the following example. Let $Ih^n(x)$ and $Ih^n(z)$ represent the x and z LVLH components of the inertial integral of CMG in-plane momentum. These terms can be generated from $h_c^n(x)$ and $h_c^n(z)$ as follows:

$$C_n^i Ih^n \triangleq \int h_c^i \, \mathrm{d}t \tag{23}$$

Differentiating

$$C_n^i \dot{I}h^n + C_n^i \Omega_{\text{in}}^n Ih^n = h_c^i \tag{24}$$

and solving for the derivative of Ih^n gives

$$\dot{I}h^n = h_c^n - \Omega_{\text{in}}^n Ih^n \tag{25}$$

By choosing $A_{11h}(1,1) = 1$, $A_{12h}(1,3) = 1$, and $A_{11\theta}(1,j) = A_{12\theta}(1,j) = 0$, $j = 1,2,3$ in Eq. (21), $f1_1(1)$ is defined as $Ih^n(x)$ and $f1_2(1)$ is defined as $Ih^n(z)$. Feedback of these states causes steady-state, zero frequency, inertial in-plane momentum error to be zero. Zeroing the inertial in-plane momentum reduces the LVLH cyclic momentum at no expense to the other plant states in steady state. It is analogous to zeroing the LVLH y axis momentum by the feedback of its integral.

All steady-state properties discussed here are achieved by any set of stabilizing feedback gains; therefore, they depend only on the definition of the filter states, not the gains.

Dynamic Torque Equilibrium Attitude

An interesting specification of filter states is $A_{0h} = A_{12h} = A_{22h} = I$ and all others set to zero. For the linearized model with disturbances at frequencies 0, ω_o, and $2\omega_o$, this results in zero closed-loop steady-state CMG torque and momentum. The spacecraft motion that results defines the "dynamic TEA," i.e., the periodic attitude motion for which no control is required even for unstable spacecraft dynamics.

If the b frame is chosen to be the principal axes of the spacecraft (i.e., $b = p$), and for this choice of b the dynamic TEA motions do not violate the small angle assumptions on θ_{np}^n, then when $T_c^n = 0$, Eqs. (18) and (19) combine to give

$$J_{11}\ddot{\theta}_x + 4(J_{22} - J_{33})\omega_o^2 \theta_x + \Delta J \omega_o \dot{\theta}_z = T_{dx}^n(t) \tag{26}$$

$$J_{22}\ddot{\theta}_y + \left[3(J_{11} - J_{33})\omega_o^2 + \overline{r_x D}\right]\theta_y + \bar{t}_{dz}\theta_x = T_{dy}^n(t) \tag{27}$$

$$J_{33}\ddot{\theta}_z + \left[(J_{22} - J_{11})\omega_o^2 + \overline{r_x D}\right]\theta_z - \Delta J \omega_o \dot{\theta}_x - \bar{t}_{dy}\theta_x = T_{dz}^n(t) \tag{28}$$

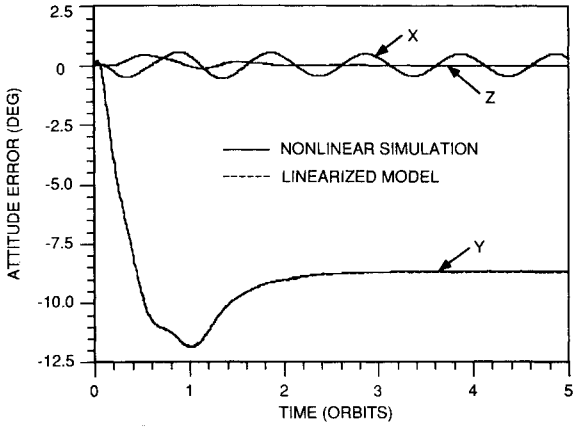

Fig. 2 Attitude errors for case 1.

where $\Delta J \triangleq J_{22} - J_{11} - J_{33}$. For a general disturbance torque defined as

$$T_d^n(t) = T_{d0} + T_{d1s}\sin(\omega_o t) + T_{d1c}\cos(\omega_o t) + T_{d2s}\sin(2\omega_o t) + T_{d2c}\cos(2\omega_o t) \quad (29)$$

where T_{d0}, T_{d1s}, T_{d1c}, T_{d2s}, and T_{d2c} are the vector coefficients of the 0, ω_o, and $2\omega_o$ components that apply when the principal axes are aligned to LVLH (i.e., $\theta_{np}^n = 0$), and with the approximation $\bar{t}_{dy} = T_{d0y}$ and $\bar{t}_{dz} = T_{d0z}$, the steady-state attitude motion of the principal axes relative to LVLH at the dynamic TEA is

$$\theta_{np}^n(t) = \theta_0 + \theta_{1s}\sin(\omega_o t) + \theta_{1c}\cos(\omega_o t) + \theta_{2s}\sin(2\omega_o t) + \theta_{2c}\cos(2\omega_o t) \quad (30)$$

where θ_0, θ_{1s}, θ_{1c}, θ_{2s}, and θ_{2c} are given in the following:

$$\theta_{0x} = T_{d0x}/\left[4(J_{22}-J_{33})\omega_o^2\right] \quad (31)$$

$$\theta_{0y} = (T_{d0y} - T_{d0z}\theta_{0x})/\left[3(J_{11}-J_{33})\omega_o^2 + \overline{r_x D}\right] \quad (32)$$

$$\theta_{0z} = (T_{d0z} + T_{d0y}\theta_{0x})/\left[(J_{22}-J_{11})\omega_o^2 + \overline{r_x D}\right] \quad (33)$$

$$\begin{bmatrix}\theta_{1sx}\\ \theta_{1cx}\\ \theta_{1sz}\\ \theta_{1cz}\end{bmatrix} = \begin{bmatrix}\left[3(J_{22}-J_{33})+\Delta J\right]\omega_o^2 & 0 & 0 & -\Delta J\omega_o^2\\ 0 & \left[3(J_{22}-J_{33})+\Delta J\right]\omega_o^2 & \Delta J\omega_o^2 & 0\\ -T_{d0y} & \Delta J\omega_o^2 & \left[\Delta J\omega_o^2 + \overline{r_x D}\right] & 0\\ -\Delta J\omega_o^2 & -T_{d0y} & 0 & \left[\Delta J\omega_o^2 + \overline{r_x D}\right]\end{bmatrix}^{-1}\begin{bmatrix}T_{d1sx}\\ T_{d1cx}\\ T_{d1sz}\\ T_{d1cz}\end{bmatrix} \quad (34)$$

$$\theta_{1sy} = (T_{d1sy} - T_{d0z}\theta_{1sx})/\left[(3J_{11}-3J_{33}-J_{22})\omega_o^2 + \overline{r_x D}\right] \quad (35)$$

$$\theta_{1cy} = (T_{d1cy} - T_{d0z}\theta_{1cx})/\left[(3J_{11}-3J_{33}-J_{22})\omega_o^2 + \overline{r_x D}\right] \quad (36)$$

$$\begin{bmatrix}\theta_{2sx}\\ \theta_{2cx}\\ \theta_{2sz}\\ \theta_{2cz}\end{bmatrix} = \begin{bmatrix}4\Delta J\omega_o^2 & 0 & 0 & -2\Delta J\omega_o^2\\ 0 & 4\Delta J\omega_o^2 & 2\Delta J\omega_o^2 & 0\\ -T_{d0y} & 2\Delta J\omega_o^2 & \left[(\Delta J - 3J_{33})\omega_o^2 + \overline{r_x D}\right] & 0\\ -2\Delta J\omega_o^2 & -T_{d0y} & 0 & \left[(\Delta J - 3J_{33})\omega_o^2 + \overline{r_x D}\right]\end{bmatrix}^{-1}\begin{bmatrix}T_{d2sx}\\ T_{d2cx}\\ T_{d2sz}\\ T_{d2cz}\end{bmatrix} \quad (37)$$

$$\theta_{2sy} = (T_{d2sy} - T_{d0z}\theta_{2sx})/\left[(3J_{11}-3J_{33}-4J_{22})\omega_o^2 + \overline{r_x D}\right] \quad (38)$$

$$\theta_{2cy} = (T_{d2cy} - T_{d0z}\theta_{2cx})/\left[(3J_{11}-3J_{33}-4J_{22})\omega_o^2 + \overline{r_x D}\right] \quad (39)$$

Similar expressions can be derived for disturbances at other frequencies.

The dynamic TEA (disturbances at frequencies 0, ω_o, and $2\omega_o$) does not exist when

1) any of the denominators in Eqs. (31-33) are zero;
2) $\Delta J = 0$;
3) $T_{d0y} = 0$ and

$$\overline{r_x D} = -3(J_{22}-J_{33})\Delta J\omega_o^2/\left[3(J_{22}-J_{33})+\Delta J\right]$$

4) the denominator in Eqs. (35) and (36) is zero; or
5) the denominator in Eqs. (38) and (39) is zero.

When any of these conditions exist, the open-loop spacecraft equations of motion will have a pair of eigenvalues at $\pm jn\omega_o$, $n = 0$, 1, or 2.

V. Numerical Examples

In all of the following examples the controller gains were calculated using linear quadratic regulator techniques. The states were scaled to avoid numerical problems, and the A matrix was then adjusted by adding 0.25 ω_o times the identity matrix to place all of the closed-loop poles to the left of a line at $-0.5\,\omega_o$. It is emphasized that the features of the controller discussed in this paper are dependent on only the architecture, and any set of stabilizing gains will result in the same steady state performance. The gains do affect transient characteristics, responses to disturbances at frequencies other than 0, ω_o, and $2\omega_o$, and robustness properties.

Case 1: Attitude Emphasis

The controller architecture can accommodate the extreme requirements to hold the steady-state attitude perfectly (causes unbounded growth of CMG momentum) or momentum perfectly (assuming the dynamic TEA exists) or any permissible combination as a function of axis and frequency. Permissible combinations are any that do not violate the laws of physics. When the primary objective in spacecraft control is minimizing attitude errors but managing momentum is still required, the controller can be configured to allow only those attitude motions required to control momentum. Since a constant offset about one axis and an orbit frequency oscillation about one axis (axes need not be LVLH cardinal axes) are required to control momentum, all other attitude errors can be held to zero. For a spacecraft having sufficient differences between its principal MOIs, a straightforward method to control momentum is by an LVLH y axis attitude offset and a sinusoidal motion at orbit frequency about the LVLH x axis. Therefore, the first example is a controller configured to allow only those attitude errors.

The spacecraft MOI and the disturbance environment, extracted from Ref. 2, correspond to the space station and are given in Table 1. The MOI are in body axes and the disturbance environment applies directly when the body axes are coincident with the LVLH frame. The combination of aerodynamic torque about the LVLH y axis and the x-z product of inertia produce a torque equilibrium attitude of -8.72 deg about the LVLH y axis. The dynamic model would normally be linearized about this operating point or the best a priori estimate of it (i.e., defining the b frame). However, to observe the sensitivity to the nonlinear terms in the equations of motion, we assume no estimate of the TEA is available and choose the b frame coincident with the body frame.

For this choice of the b frame the matrix $A_{H\theta}$ is

$$A_{H\theta} = \begin{bmatrix}3.03 & -0.02 & -0.01\\ -0.04 & 0.53 & -0.01\\ 0.07 & 0.0 & 0.0\end{bmatrix} \quad \text{ft-lb/deg}$$

Table 2 Gain matrix (transpose) for case 1

0.50944E−02	−0.44536E−04	0.33915E−02
−0.61732E−04	0.58705E−02	−0.13872E−03
0.31546E−03	0.52624E−04	0.17262E−02
0.13173E+04	−0.13782E+02	0.46294E+03
−0.95633E+01	0.35004E+03	−0.34238E+01
0.78325E+02	−0.79062E+01	0.86607E+03
0.12265E−01	−0.38229E−04	0.43548E−02
−0.55426E−04	0.14060E−01	−0.16916E−03
0.12787E−02	0.22181E−04	0.74622E−02
0.20567E+00	0.33468E−02	0.14341E+00
−0.26166E−08	0.11287E−05	−0.28835E−07
−0.61602E−01	0.14200E−02	0.64891E−01
0.93355E−06	−0.82028E−08	0.25620E−06
−0.17475E−03	0.28069E−01	−0.23830E−02
0.27390E−01	−0.21999E−02	−0.25403E+00
−0.15642E−06	0.84355E−08	0.48400E−06
0.15690E−04	0.14518E+00	−0.64132E−03
−0.12221E+00	−0.20873E−02	0.14046E+00
−0.14074E+00	−0.20184E−02	0.15021E+00
0.10741E−02	−0.91555E−02	−0.36546E−02
−0.14822E−01	−0.27602E−02	−0.48266E+00
0.45520E+00	−0.11973E−02	0.61600E+00
−0.38273E−02	0.16069E+00	−0.51243E−02
−0.18086E+00	−0.13413E−02	0.28227E+00

Table 3 Closed-loop eigenvalues for case 1

Eigenvalues normalized by ω_o			
Real	Imag.	Real	Imag.
−0.5000	±0.0000	−1.5231	±0.3374
−0.5001	±0.0073	−1.3426	±1.1687
−0.4994	±0.9878	−0.5000	±2.0000
−0.5000	±1.0000	−0.5001	±2.0000
−0.5001	±1.0000	−0.5001	±2.0000
−0.5013	±1.0122	−2.2225	±1.2354

In-plane momentum control will be accomplished by motion about the LVLH x axis using the $A_{H\theta}(1, 1)$ term, and out-of-plane momentum control will be accomplished by an offset about the LVLH y axis using the $A_{H\theta}(2, 2)$ term.

The augmented states are defined by the following matrices:

$$A_{0h} = \begin{bmatrix} 0 & 0 & 0 \\ 0 & 1 & 0 \\ 0 & 0 & 0 \end{bmatrix}, \quad A_{0\theta} = \begin{bmatrix} 1 & 0 & 0 \\ 0 & 0 & 0 \\ 0 & 0 & 1 \end{bmatrix}$$

$$A_{11h} = \begin{bmatrix} 1 & 0 & 0 \\ 0 & 0 & 0 \\ 0 & 0 & 0 \end{bmatrix}, \quad A_{11\theta} = \begin{bmatrix} 0 & 0 & 0 \\ 0 & 0 & 0 \\ 0 & 0 & 0 \end{bmatrix}$$

$$A_{12h} = \begin{bmatrix} 0 & 0 & 1 \\ 0 & 0 & 0 \\ 0 & 0 & 0 \end{bmatrix}, \quad A_{12\theta} = \begin{bmatrix} 0 & 0 & 0 \\ 0 & 1 & 0 \\ 0 & 0 & 1 \end{bmatrix}$$

$$A_{21h} = \begin{bmatrix} 0 & 0 & 0 \\ 0 & 0 & 0 \\ 0 & 0 & 0 \end{bmatrix}, \quad A_{21\theta} = \begin{bmatrix} 0 & 0 & 0 \\ 0 & 0 & 0 \\ 0 & 0 & 0 \end{bmatrix}$$

$$A_{22h} = \begin{bmatrix} 0 & 0 & 0 \\ 0 & 0 & 0 \\ 0 & 0 & 0 \end{bmatrix}, \quad A_{22\theta} = \begin{bmatrix} 1 & 0 & 0 \\ 0 & 1 & 0 \\ 0 & 0 & 1 \end{bmatrix}$$

This definition constrains attitude completely except the LVLH y axis at zero frequency and the LVLH x axis at orbit frequency. The momentum entries make the zero-frequency component of inertial momentum zero in all axes.

For this specification of plant parameters and augmented states, the controller gains, computed as described earlier, are given in Table 2, and the closed-loop poles are given in Table 3.

All states were initialized to zero and the disturbances applied. The attitude response of the system, including the nonlinear dynamics, is shown in Fig. 2. The attitude quantities plotted are one-half the differences between the off-diagonal terms of the direction cosine matrix C_b^n, which, to first order, are the same as twice the vector elements of the equivalent quaternion. The linearized model was run simultaneously and its outputs are also on the plot. In steady state the only attitude errors are a constant LVLH y axis attitude error and a zero mean sinusoid at orbit frequency along the LVLH x axis as desired. The corresponding LVLH CMG momentum is shown in Fig. 3, and the inertial in-plane momentum is shown in Fig. 4. The inertial momentum has zero mean in each axis as desired.

Choosing the b frame to be the body frame (equations were linearized about a point 8.7 deg away from the average steady-state orientation) did not produce any significant differences between the linearized model and the nonlinear simulation for this case.

Case 2: Momentum Emphasis: Dynamic Torque Equilibrium Attitude

This example demonstrates the controller's ability to seek and maintain the dynamic TEA. The spacecraft MOI and disturbance environment are identical to those in case 1. Using Eqs. (31–39) and assuming $\overline{r_x D} = 0$ (center of pressure lies in the y-z plane), we determine that the dynamic TEA exists and

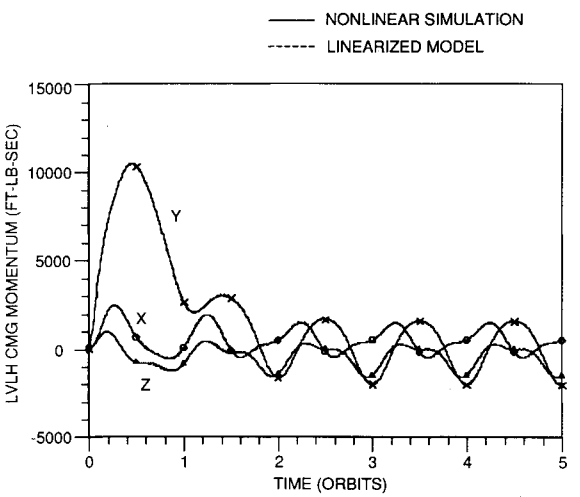

Fig. 3 LVLH CMG momentum for case 1.

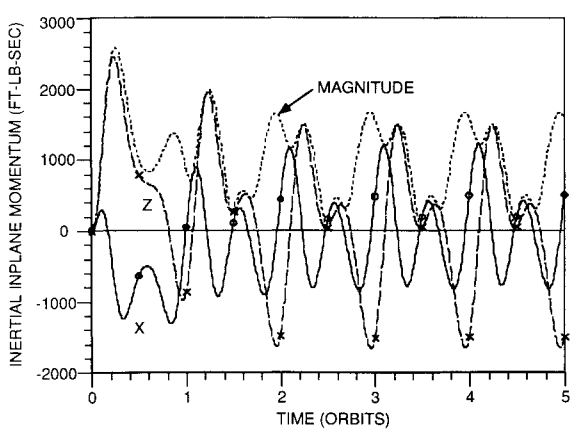

Fig. 4 Inertial in-plane CMG momentum has zero mean (case 1).

Table 4 Gain matrix (transpose) for case 2

0.76733E−02	0.58114E−05	0.33503E−02
0.18870E−04	0.11187E−01	−0.15110E−03
−0.31897E−02	0.76886E−04	0.59561E−02
0.11561E+04	−0.13316E+02	0.63861E+03
−0.83826E+01	0.35508E+03	−0.63988E+01
0.69357E+02	−0.13781E+02	0.52646E+03
0.14844E−01	0.12118E−04	0.43136E−02
0.25177E−04	0.19377E−01	−0.18154E−03
−0.22264E−02	0.46444E−04	0.11692E−01
−0.14013E−05	0.32944E−07	0.15048E−05
−0.26073E−08	0.11287E−05	−0.28832E−07
−0.10025E−05	−0.15395E−07	−0.65811E−06
0.41378E−06	−0.55909E−07	−0.28430E−05
−0.12140E−07	−0.37016E−05	0.30902E−07
0.20651E−05	−0.67697E−08	−0.10376E−05
−0.19876E−06	−0.96269E−08	0.15495E−05
−0.64643E−08	0.71602E−06	−0.37280E−07
0.10127E−06	−0.39058E−07	−0.18754E−05
−0.21218E−05	−0.32965E−07	−0.28351E−05
−0.92093E−08	−0.42929E−05	0.28625E−07
0.11765E−05	0.88083E−08	−0.19502E−05
−0.67370E−06	−0.18297E−07	0.71363E−06
0.21383E−08	−0.24523E−06	−0.25331E−07
0.60023E−06	−0.38732E−07	−0.27904E−05

Table 5 Closed-loop eigenvalues for case 2

Eigenvalues normalized by ω_o			
Real	Imag.	Real	Imag.
−0.5001	±0.0000	−1.5231	±0.3374
−0.5002	±0.0073	−1.3426	±1.1687
−0.4996	±0.9913	−0.5000	±2.0000
−0.5000	±1.0000	−0.5001	±2.0000
−0.5000	±1.0000	−0.5002	±2.0001
−0.5010	±1.0086	−2.2225	±1.2354

is approximated by the following motion of the principal axes relative to LVLH:

$$\theta^n_{np}(t) = \begin{bmatrix} -0.25 \\ -7.62 \\ -1.18 \end{bmatrix} + \begin{bmatrix} -0.34 \\ -2.66 \\ -0.79 \end{bmatrix} \sin(\omega_o t) + \begin{bmatrix} 0.32 \\ 0.01 \\ -0.35 \end{bmatrix} \cos(\omega_o t) + \begin{bmatrix} -0.09 \\ -0.35 \\ -0.13 \end{bmatrix} \sin(2\omega_o t) + \begin{bmatrix} 0.07 \\ 0.00 \\ -0.07 \end{bmatrix} \cos(2\omega_o t) \quad \text{(deg)} \tag{40}$$

The augmented states for this example are defined as in the dynamic TEA discussion in Sec. IV. Again, we choose the b frame to be the body frame. A better linearization would be obtained by choosing the b frame based on the constant term in Eq. (40) together with the known principal axis offsets. Incorrectly choosing the linearization point can produce differences between the linearized model and actual responses. However, if the gains (calculated based on the linearized model) stabilize the system, the desired steady-state performance is still achieved.

The controller gains are given in Table 4, and the closed-loop eigenvalues are given in Table 5. Figure 5 shows the resulting attitude response—the dynamic TEA. The LVLH CMG momentum is shown in Fig. 6. Following the transient there is no evidence of any momentum error at frequencies below $3\omega_o$. The error at $3\omega_o$ (not visible on this scale) is caused by nonlinear terms in the equations of motion involving products of angular rates having harmonic content at ω_o and $2\omega_o$.

Case 3: Equal x- and z-Axis Moments of Inertia

This example demonstrates gravity gradient momentum control for a spacecraft having equal x- and z-axis principal moments of inertia. The inertia tensor is diagonal with elements 58.57, 10.80, and 58.57×10^6 slug-ft^2 for the x, y, and z body axes, respectively. This spacecraft cannot produce gravity gradient torque about the LVLH y axis when its x and z body axes are constrained to lie in the orbit plane. However, if the spacecraft is given a constant offset about the z axis,

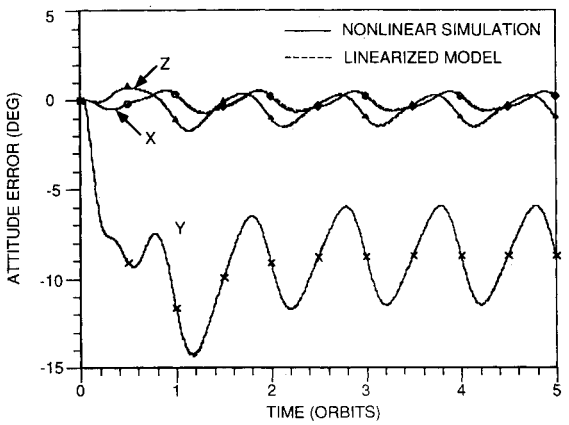

Fig. 5 Dynamic TEA (case 2).

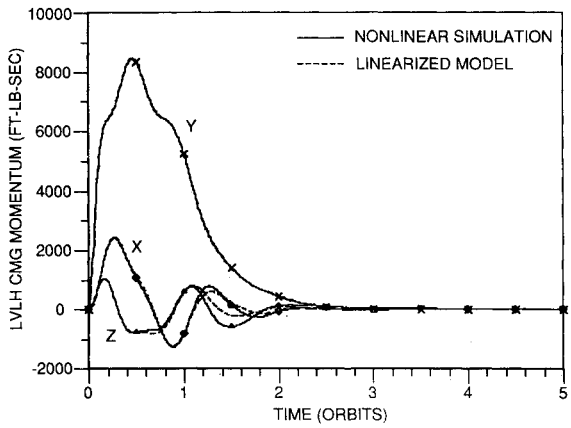

Fig. 6 LVLH CMG momentum at the dynamic TEA (case 2).

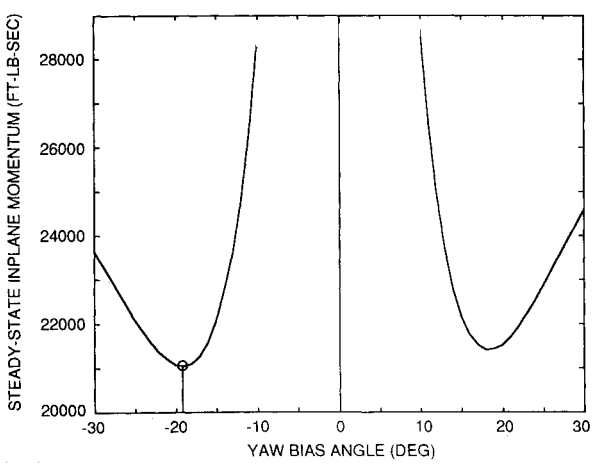

Fig. 7 Magnitude of steady-state CMG momentum vs yaw bias angle.

then gravity gradient torques can be produced to control momentum by body roll motion of the spacecraft.

The optimum offset for the disturbance environment specified in Table 1 (in terms of minimizing CMG steady-state torque and momentum) is approximately -19 deg and is obtained from Fig. 7. Figure 7 was generated by computing the body roll angle necessary to achieve LVLH y-axis torque equilibrium for various yaw angles and then computing the in-plane torque and momentum required to sustain that orientation. For this offset, a constant body axis roll angle of $+4.0$ deg is required to achieve LVLH y-axis torque equilibrium. All momentum control in this example is performed with rotations about only the body x axis. The b frame was chosen to be coincident with the LVLH frame when the spacecraft is yawed -19 deg about the LVLH z axis. The LVLH external torques due to body axis motions are given by

$$A_{H\theta}C^{b}_{\text{body}} = \begin{bmatrix} 2.86 & 0.0 & 0.0 \\ -1.00 & -0.01 & 0.0 \\ 0.07 & 0.02 & -0.01 \end{bmatrix} \quad \text{ft-lb/deg}$$

and it is clear that body roll motions have the dominant effect for in-plane and out-of-plane momentum control.

The augmented state definitions for this case are

$$A_{0h} = \begin{bmatrix} 0 & 0 & 0 \\ 0 & 1 & 0 \\ 0 & 0 & 0 \end{bmatrix} \quad A_{0\theta} = \begin{bmatrix} 0.3256 & 0.9455 & 0 \\ 0 & 0 & 0 \\ 0 & 0 & 1 \end{bmatrix}$$

$$A_{11h} = \begin{bmatrix} 1 & 0 & 0 \\ 0 & 0 & 0 \\ 0 & 0 & 0 \end{bmatrix} \quad A_{11\theta} = \begin{bmatrix} 0 & 0 & 0 \\ 0 & 0 & 0 \\ 0 & 0 & 0 \end{bmatrix}$$

$$A_{12h} = \begin{bmatrix} 0 & 0 & 1 \\ 0 & 0 & 0 \\ 0 & 0 & 0 \end{bmatrix} \quad A_{12\theta} = \begin{bmatrix} 0 & 0 & 0 \\ 0.3256 & 0.9455 & 0 \\ 0 & 0 & 1 \end{bmatrix}$$

$$A_{21h} = \begin{bmatrix} 0 & 0 & 0 \\ 0 & 0 & 0 \\ 0 & 0 & 0 \end{bmatrix} \quad A_{21\theta} = \begin{bmatrix} 0 & 0 & 0 \\ 0 & 0 & 0 \\ 0 & 0 & 0 \end{bmatrix}$$

$$A_{22h} = \begin{bmatrix} 0 & 0 & 0 \\ 0 & 0 & 0 \\ 0 & 0 & 0 \end{bmatrix} \quad A_{22\theta} = \begin{bmatrix} 1 & 0 & 0 \\ 0 & 1 & 0 \\ 0 & 0 & 1 \end{bmatrix}$$

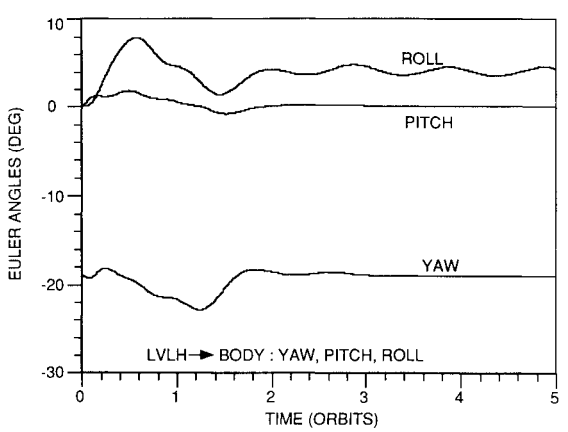

Fig. 8 Spacecraft attitude for equal x and z MOI (case 3).

Table 6 Gain matrix (transpose) for case 3

0.59848$E-02$	−0.21943$E-02$	0.45861$E-02$
−0.96741$E-02$	0.34809$E-02$	−0.92053$E-02$
−0.13864$E-02$	0.48216$E-03$	−0.18379$E-03$
0.14354$E+04$	−0.41660$E+03$	0.65741$E+03$
−0.43183$E+03$	0.37555$E+03$	−0.22449$E+03$
0.11713$E+03$	−0.18749$E+03$	0.93741$E+03$
0.13045$E-01$	−0.23395$E-02$	0.57395$E-02$
−0.98193$E-02$	0.10308$E-01$	−0.96433$E-02$
−0.23306$E-03$	0.44217$E-04$	0.58063$E-02$
0.15126$E-01$	0.53171$E-01$	0.23139$E-02$
−0.15851$E-05$	0.55192$E-06$	−0.16624$E-05$
−0.88586$E-01$	0.27505$E-01$	0.32617$E-01$
0.10331$E-05$	−0.36691$E-06$	0.37402$E-06$
−0.15138$E-01$	−0.23245$E-01$	−0.53832$E-02$
0.36899$E-01$	−0.57059$E-02$	−0.25180$E+00$
−0.41002$E-06$	0.13488$E-06$	0.21916$E-06$
0.35659$E-01$	0.10355$E+00$	0.10430$E-01$
−0.67295$E-01$	0.13068$E-01$	0.19053$E+00$
−0.63160$E-01$	−0.32156$E-02$	0.26789$E+00$
0.64760$E-02$	−0.40246$E-01$	−0.89637$E-01$
0.41775$E-02$	0.38043$E-02$	−0.47277$E+00$
0.44180$E+00$	−0.12415$E+00$	0.62266$E+00$
−0.11399$E+00$	0.16394$E+00$	−0.20201$E+00$
−0.12709$E+00$	0.25162$E-01$	0.33873$E+00$

Table 7 Closed-loop eigenvalues for case 3

Eigenvalues normalized by ω_o			
Real	Imag.	Real	Imag.
−0.5000	±0.0044	−1.4387	±0.3333
−0.5002	±0.0000	−1.2723	±1.1621
−0.4992	±0.9884	−0.5000	±2.0000
−0.5000	±1.0000	−0.5000	±2.0000
−0.5002	±1.0000	−0.5002	±2.0000
−0.5015	±1.0116	−1.8225	±1.5733

Table 8 Gain matrix (transpose) for case 4

0.29653$E-01$	−0.32909$E-02$	−0.61929$E-01$
−0.12399$E-01$	0.77509$E-02$	−0.52199$E-02$
0.60329$E-02$	0.81278$E-03$	0.19264$E-01$
0.98831$E+03$	−0.11345$E+03$	−0.20453$E+02$
−0.17662$E+03$	0.83448$E+03$	−0.71333$E+02$
−0.45709$E+03$	0.26034$E+02$	0.12385$E+04$
0.34888$E-01$	−0.36046$E-02$	−0.62237$E-01$
−0.12712$E-01$	0.13005$E-01$	−0.53480$E-02$
0.57250$E-02$	0.68468$E-03$	0.24831$E-01$
0.66411$E-01$	0.68408$E-01$	0.29330$E-01$
−0.15769$E-05$	0.18348$E-05$	−0.63174$E-06$
−0.31339$E-01$	−0.17965$E-02$	0.83765$E-01$
0.47696$E-05$	−0.15629$E-06$	−0.34612$E-05$
−0.45661$E+00$	−0.22090$E-01$	0.19898$E+00$
−0.21945$E-01$	−0.14161$E+00$	−0.86923$E-02$
−0.19415$E-05$	0.73235$E-06$	0.67845$E-05$
0.27729$E+00$	−0.99444$E-01$	−0.34097$E+00$
−0.43311$E-01$	0.16248$E+00$	−0.17683$E-01$
−0.38757$E+00$	−0.26856$E-01$	−0.89364$E-02$
−0.16139$E-01$	−0.37867$E+00$	−0.64482$E-02$
−0.25531$E-01$	0.22035$E-01$	−0.28395$E+00$
0.22613$E+00$	−0.59398$E-01$	0.14457$E+00$
−0.55598$E-01$	0.23310$E+00$	−0.22742$E-01$
−0.29781$E+00$	−0.20191$E-01$	0.30514$E+00$

Table 9 Closed-loop eigenvalues for case 4

Eigenvalues normalized by ω_o			
Real	Imag.	Real	Imag.
−0.4999	±0.0022	−0.5033	±1.0024
−0.5003	±0.0000	−1.0043	±0.5901
−0.9000	±0.2248	−0.8930	±1.2245
−0.4969	±0.9975	−0.5000	±2.0000
−0.5000	±1.0000	−0.5000	±2.0000
−0.5000	±1.0000	−0.5000	±2.0000

The nonzero rows of $A_{0\theta}$ and $A_{12\theta}$ are unit vectors orthogonal to the body x axis, components in LVLH. This will permit steady-state attitude errors only about the body x axis. The momentum entries will produce zero mean inertial momentum. The gains are given in Table 6, and the closed-loop poles for this case are given in Table 7. The states were initialized to zero and the disturbances were applied. Figure 8 contains the LVLH to body Euler angles (sequence: yaw, pitch, roll from LVLH to body), and it is seen that in steady state there is a constant yaw offset of -19 deg, pitch is zero, and roll consists of a 4.0-deg bias plus a sinusoid at orbit frequency. The corresponding LVLH CMG momentum is shown in Fig. 9. The large momentum offsets in the x and z axes are due to the large CMG torques required to sustain the spacecraft orientation (due to gyroscopic and LVLH x-axis gravity gradient torques). This would be a practical method of momentum management for this spacecraft if it possessed sufficient CMG torque and momentum capability and the attitude offsets were permissible.

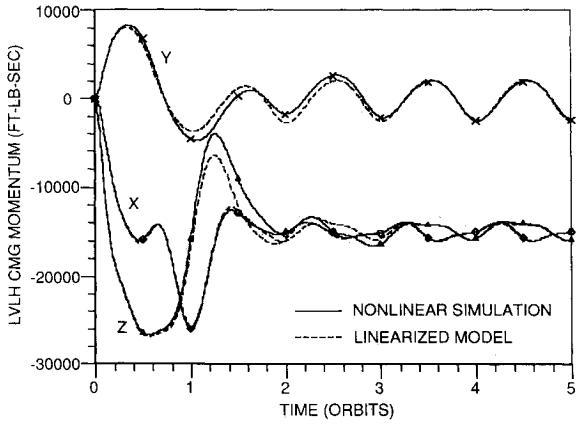

Fig. 9 LVLH CMG momentum for case 3.

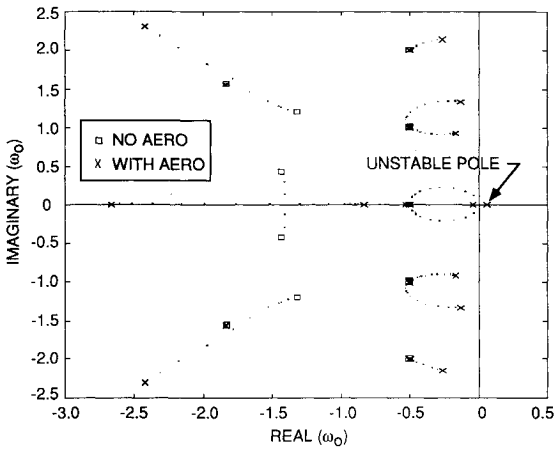

Fig. 10 Ignoring aerodynamic torque derivatives results in unstable design.

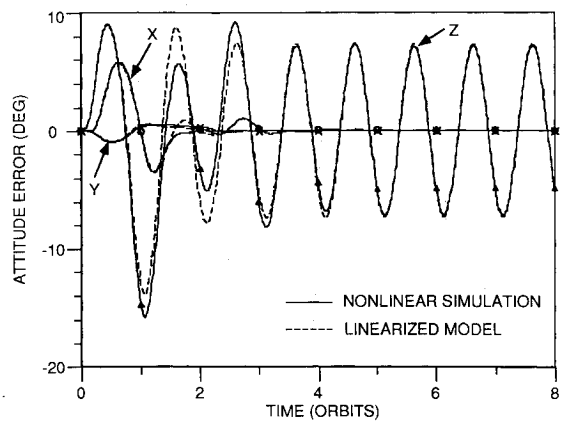

Fig. 11 Attitude errors for spherical MOI (case 4).

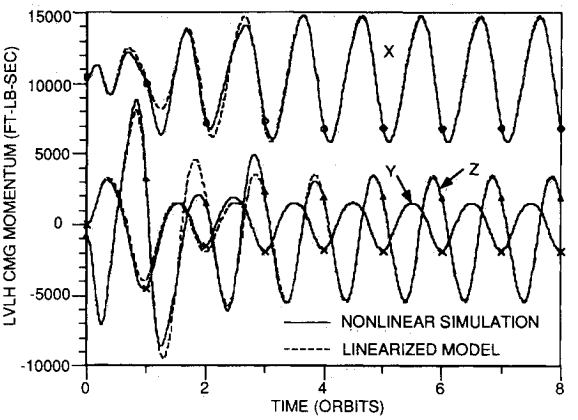

Fig. 12 LVLH CMG momentum for case 4.

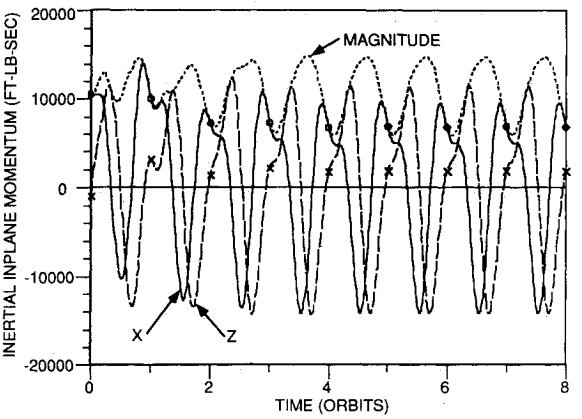

Fig. 13 Inertial in-plane CMG momentum has zero mean (case 4).

The importance of including the aerodynamic torque derivatives in the controller design is illustrated in the following. Using the same MOI as that given earlier and repeating that procedure, a controller was designed for a $+5$ deg yaw bias. This time, however, the aerodynamic torque derivatives were ignored. The constant component of the disturbance torque was set to $[1\ 2\ 16]^T$ ft-lb instead of the $[1\ 4\ 1]^T$ ft-lb used earlier. Such a torque could result from a stalled alpha gimbal solar array drive on the space station. Figure 10 shows the closed-loop poles for this design when the aerodynamic torque derivatives are left out of the model. This appears to be a good design having all poles at least $0.5\omega_o$ into the left half plane. However, when the aerodynamic torque derivatives are included in the model, the system becomes unstable (also shown in Fig. 10). This is because for these parameter values the LVLH y-axis aerodynamic torque derivative with respect to body roll motion (-0.275 ft-lb/deg) has the opposite sign to, and is larger than, the corresponding gravity gradient torque derivative (0.264 ft-lb/deg).

Case 4: Spherical Moment of Inertia

To demonstrate the capability to use aerodynamic torques for momentum management, let the spacecraft have the MOI properties of a sphere, all principal MOIs equal to 57.58×10^6 slug-ft^2. No gravity gradient torques can be produced. Let the constant components of the disturbance torque be $[1\ 2\ 16]^T$ when the spacecraft body axes are aligned to LVLH and as-

sume the aerodynamic center of pressure lies in the body y-z plane. By allowing a yaw attitude bias, momentum can be controlled by an offset about the LVLH x axis and a sinusoidal motion about the LVLH z axis at orbit frequency. All other motions can be held to zero. An arbitrarily selected yaw bias of -45 deg places the center of pressure forward of the spacecraft center of mass (unstable in pitch and yaw) and allows z-axis motions to modulate the yaw aerodynamic torque. A constant offset of $+10.03$ deg about the LVLH x axis places the body in torque equilibrium about the LVLH y axis and defines the b frame:

$$C^b_{\text{body}} = \begin{bmatrix} 0.7071 & 0.7071 & 0 \\ -0.6963 & 0.6963 & -0.1741 \\ -0.1231 & 0.1231 & 0.9847 \end{bmatrix}$$

By specifying the augmented states with

$$A_{0h} = \begin{bmatrix} 0 & 0 & 0 \\ 0 & 1 & 0 \\ 0 & 0 & 0 \end{bmatrix}, \quad A_{0\theta} = \begin{bmatrix} 0 & 1 & 0 \\ 0 & 0 & 0 \\ 0 & 0 & 1 \end{bmatrix}$$

$$A_{11h} = \begin{bmatrix} 1 & 0 & 0 \\ 0 & 0 & 0 \\ 0 & 0 & 0 \end{bmatrix}, \quad A_{11\theta} = \begin{bmatrix} 0 & 0 & 0 \\ 0 & 0 & 0 \\ 0 & 0 & 0 \end{bmatrix}$$

$$A_{12h} = \begin{bmatrix} 0 & 0 & 1 \\ 0 & 0 & 0 \\ 0 & 0 & 0 \end{bmatrix}, \quad A_{12\theta} = \begin{bmatrix} 0 & 0 & 0 \\ 1 & 0 & 0 \\ 0 & 1 & 0 \end{bmatrix}$$

$$A_{21h} = \begin{bmatrix} 0 & 0 & 0 \\ 0 & 0 & 0 \\ 0 & 0 & 0 \end{bmatrix}, \quad A_{21\theta} = \begin{bmatrix} 0 & 0 & 0 \\ 0 & 0 & 0 \\ 0 & 0 & 0 \end{bmatrix}$$

$$A_{22h} = \begin{bmatrix} 0 & 0 & 0 \\ 0 & 0 & 0 \\ 0 & 0 & 0 \end{bmatrix}, \quad A_{22\theta} = \begin{bmatrix} 1 & 0 & 0 \\ 0 & 1 & 0 \\ 0 & 0 & 1 \end{bmatrix}$$

a controller was designed that constrains the motion as desired and controls the momentum. The gains are given in Table 8, and the closed-loop eigenvalues are given in Table 9. The states were initialized to their mean steady-state values, and the disturbances were applied. Figure 11 shows the attitude error of the b frame relative to LVLH, and Fig. 12 shows the LVLH CMG momentum history. The LVLH x-axis momentum offset is due to the LVLH z-axis CMG torque required to cancel the constant component of the aerodynamic torque. Figure 13 shows that the in-plane inertial CMG momentum components have zero mean as desired.

VI. Conclusion

A three-axis coupled controller architecture has been developed for momentum management of Earth-oriented spacecraft that automatically generates gravity gradient and aerodynamic torques required for momentum control by maneuvering the spacecraft. This architecture lets the designer selectively suppress the steady-state effects of constant or periodic disturbances in the attitude or momentum states. The designer may specify the attitude offsets and motions used for momentum control by suppressing the other attitude states. The coupled nature of the controller permits momentum control of spacecraft having equal principal moments of inertia or significant pitch-to-roll/yaw coupling. The method presented for inertial momentum centering reduces cyclic control moment gyro momentum use with no penalty on the steady-state attitude states.

References

[1]Shain, E. B., and Spector, V. A., "Adaptive Torque Equilibrium Control of the Space Station," AIAA Paper 85-0028, Jan. 1985.

[2]Wie, B., et al., "A New Momentum Management Controller for the Space Station," *Journal of Guidance, Control, and Dynamics,* Vol. 12, No. 5, 1989, pp. 714–722.

[3]Warren, W., Wie, B., and Geller, D., "Periodic-Disturbance Accommodating Control of the Space Station for Asymptotic Momentum Management," *Journal of Guidance, Control, and Dynamics,* Vol. 13, No. 6, 1990, pp. 984–992.

[4]Sunkel, J. W., and Shieh, L. S., "An Optimal Momentum Management Controller for the Space Station," *Proceedings of the AIAA Guidance, Navigation, and Control Conference* (Boston, MA), AIAA, Washington, DC, 1989, Pt. 1, p. 402 (AIAA Paper 89-3473).

[5]Sunkel, J. W., and Shieh, L. S., "Digital Redesign of an Optimal Momentum Management Controller for the Space Station," *Proceedings of the AIAA Guidance, Navigation, and Control Conference* (Boston, MA), AIAA, Washington, DC, 1989, Pt. 1, p. 412 (AIAA Paper 89-3474).

[6]Miller, P. A., "Torque Equilibirum Control of Low Altitude Spacecraft," *Proceedings of the AIAA Guidance, Navigation, and Control Conference* (Monterey, CA), AIAA, Washington, DC, 1987 (AIAA Paper 87-2532).